# Neutron Diffraction and the Magnetic Structure of $TlMnCl_3$

M. Melamud, H. Pinto, G. Shachar, J. Makovsky, and H. Shaked
*Nuclear Research Centre, Negev, P.O.B. 9001, Beer-Sheva, Israel*
(Received 14 September 1970)

Neutron-diffraction and magnetic-susceptibility measurements show that $TlMnCl_3$ is an antiferromagnet of type $G$ with $T_N = 118\,^\circ$K. A transition to weak ferromagnetism is observed at about 108 °K. Reflections in the neutron-diffraction pattern at 330 °K correspond to the undistorted cubic perovskite with $a_0 = 5.02$ Å. As temperature is lowered below 330 °K, superlattice lines appear in the neutron-diffraction pattern. An analysis of these lines, assuming the symmetry *Pbnm*, indicated that the lines are due to a distortion of the $Cl^-$ octahedra.

## I. INTRODUCTION

Many ionic compounds of the formula $ABX_3$ crystallize in the perovskite structure. The $B$ ions are accommodated in the holes between the close-packed $AX_3$ layers. In the case that the $B$ ions are paramagnetic, magnetic ordering may occur, and has indeed been observed in many perovskitelike double-metal oxides of trivalent $3d$ ions,[1] and in double-metal fluorides of divalent $3d$ ions.[2] Some compounds of the corresponding double-metal chlorides have also been investigated.[3] Recently, $TlMnCl_3$ was prepared,[4] and its structure above 300 °K was found to be the ideal perovskite structure. In the present paper we report the results of a study of magnetic properties of $TlMnCl_3$ using neutron-diffraction and magnetic-susceptibility measurements on polycrystalline samples. In addition, a temperature-dependent distortion of the chlorine octahedra was found and is described.

## II. PREPARATION OF SAMPLES AND MAGNETIC MEASUREMENTS

Stoichiometric amounts of TlCl and anhydrous $MnCl_2$ were weighed into a quartz ampoule which was sealed after evacuation. All weighings and sample preparations were carried out in a dry argon atmosphere. The sealed ampoule was heated up to 520 °C [the melting point of $TlMnCl_3$ is (497 ± 5) °C] and left at this temperature for a few hours.

TABLE I. Observed and calculated integrated intensities for $TlMnCl_3$ at 330 °K. Indices correspond to the cubic perovskite cell with $a_0 = 5.02$ Å.

| $\{hkl\}$ | $I_{obs}$ | $I_{calc}$ |
|---|---|---|
| 100 | 1.1 | 0.4 |
| 110 | 1.7 | 1.4 |
| 111 | 46.2 | 46.4 |
| 200 | 15.3 | 16.2 |
| 210 | 0.3 | 0.3 |
| 220 | 11.6 | 12.8 |
| 310 | 1.0 | 0.3 |
| 311 | 22.8 | 22.1 |

The color of the resulting material was orange. Chemical analysis of the manganese ion was carried out by the ethylene-diamine tetra-acetic acid complexometric titration, and that of the chlorine ion by argentometric titration. The results of the chemical analysis are $Mn^{+2}$, 14.9 wt% (theor, 15.01) and $Cl^-$, 29.0 wt% (theor, 29.09). Magnetic measurements on polycrystalline $TlMnCl_3$ were performed with a vibrating-sample magnetometer (VSM). A transition to antiferromagnetism is observed at (120 ± 5) °K. In addition a transition to weak ferromagnetism is observed at about 108 °K.

## III. NEUTRON DIFFRACTION

Neutron-diffraction patterns ($\lambda \sim 1.02$ Å) of polycrystalline $TlMnCl_3$ at 330, 272, and 77 °K are presented in Fig. 1. The 330 °K data are consistent with an undistorted cubic perovskite structure, with $a_0 = 5.02$ Å, having one formula unit per unit cell. The cubic indices are indicated at the top of the figure. The observed integrated intensities are compared in Table I with the intensities calculated for the ideal cubic perovskite. The $R$ factor[5] was minimized with respect to the Debye-Waller factor $B$.[6] This minimalization yielded 4.7% and 3.5 $Å^2$ for $R$ and $B$, respectively. In the 272 °K spectrum [Fig. 1(b)] several additional peaks are observed. All these peaks correspond to superlattice reflections and can be indexed on a cubic unit cell with $a = 2a_0$ containing eight formula units, or on a tetragonal cell with $a = b = a_0\sqrt{2}$, $c = 2a_0$ containing only four formula units. The latter indexing is given at the bottom of Fig. 1(c). In this and Sec. IV these tetragonal indices will be used. In the 77 °K pattern [Fig. 1(c)] an increase in the intensities of the superlattice lines is observed. The temperature dependence of three of the superlattice lines is shown in Fig. 2. A transition temperature of (118 ± 2) °K is deduced from the temperature dependence of the peak intensity of the {101} line [Fig. 2(a)]. The temperature dependence of the peak intensity at $2\theta = 34°50'$ is presented in Fig. 2(c). As the temperature is raised from 77 °K the intensity decreases gradually, almost linearly.

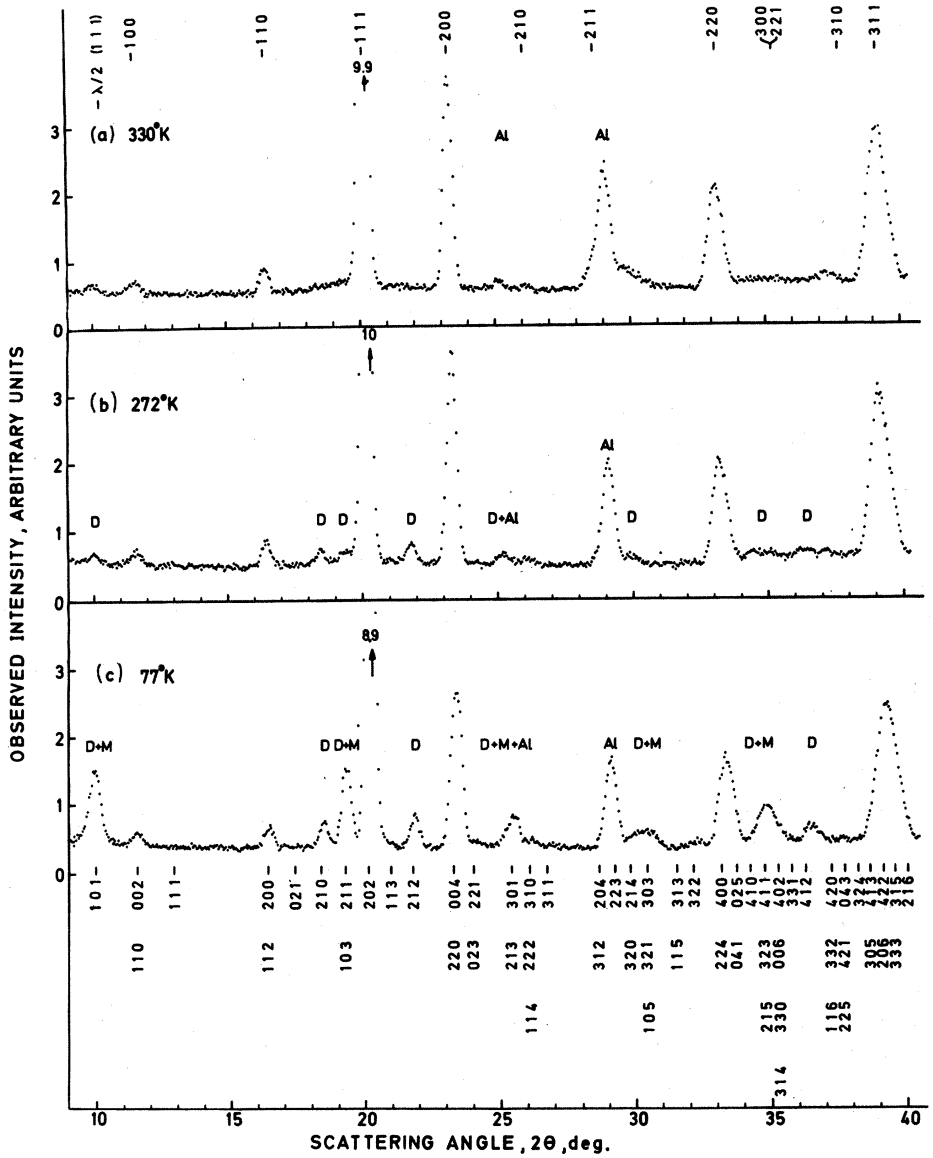


FIG. 1. Neutron-diffraction patterns ($\lambda = 1.02$ Å) of $TlMnCl_3$. (a) At 330 °K the indices correspond to the cubic perovskite cell with $a_0 = 5.02$ Å. (b) At 272 °K the distortion lines are labeled D. (c) At 77 °K the magnetic contributions are labeled M. The indices correspond to the tetragonal crystallographic cell with $a = b = 5.02 \times \sqrt{2}$ Å, $c = 5.02 \times 2$ Å. Lines from the aluminum sample holder are labeled Al.

The temperature dependence of the peak intensity at $2\theta = 19°20'$ is more complex: A transition temperature of $(118 \pm 2)$ °K is followed by a linear decrease in the intensity towards the higher temperature. On the basis of these data and the VSM results mentioned in Sec. II we have concluded that the "nonlinear" part in the temperature dependence of the lines in Fig. 2 is due to a magnetic contribution. As for the "linear" parts in Fig. 2, we stipulate that they are due to temperature-dependent parameters of the ionic sites, an effect which we shall refer to as "distortion." We have accordingly labeled the lines in Fig. 1 by D and M for distortion and magnetic contributions, respectively. In order to distinguish between these contributions, a magnetic field of 6 kG was applied to the sample parallel to the scattering vector. The results are presented in Table II. For the two lines {101} and {211}+{103}, the magnetic contributions (see below) were the major part of the intensities at 77 °K (compare Fig. 2). For these two lines the application of the magnetic field resulted in an increase of over 40% in the magnetic contributions. The changes observed for the other reflections are smaller and most of them are statistically insignificant. No hysteresis was observed; after turning off the field the counts dropped to their prefield value. The application of the magnetic field to the sample at room temperature yielded only statistically insignificant changes.

## IV. DISCUSSION

The results presented above show that both magnetic and distortion effects are manifested in the low-temperature data of $TlMnCl_3$. The magnetic

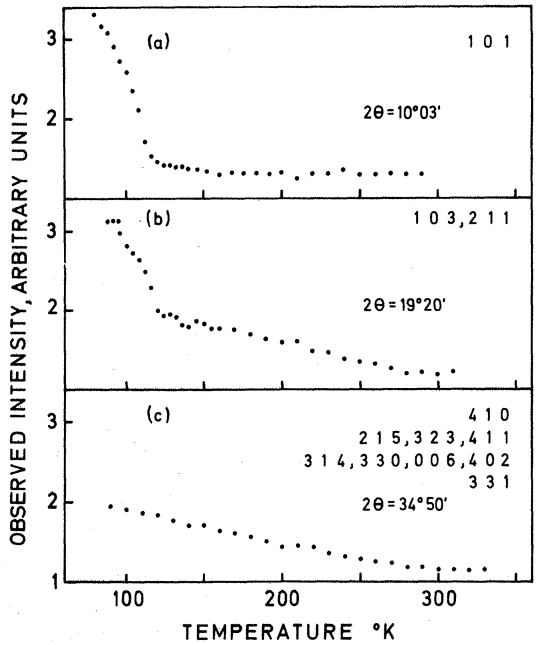


FIG. 2. Temperature dependence of the lines (a) at $2\theta = 10°3'$; (b) at $2\theta = 19°20'$; (c) at $2\theta = 34°50'$. Each group of three numbers denotes the planes from which the reflected intensity is observed.

ordering will be discussed first. The transition temperature deduced from the neutron-diffraction pattern, $(118 \pm 2)$ °K, agrees with the Néel temperature of $(120 \pm 5)$ °K found using the VSM. The peak intensity of the {101} line in the range 4.2–300 °K is presented in Fig. 3 in a reduced form. The corresponding reduced magnetization, calculated in the molecular-field approximation for $J = \frac{5}{2}$, is also shown. The comparison shows that the {101} line is mainly magnetic. In discussing the corresponding magnetic mode we note that in many distorted perovskites (e.g., the orthoferrites) the magnetic $B$ ions retain their ideal positions.[7] Also, for $TlMnCl_3$ the calculations presented below show that the neutron-diffraction data are fully consistent with a unit cell in which the manganese ions retain their ideal positions. The occurrence of magnetic reflections like {101} and {211}+{103}, which are characterized by $h+k$ odd and $l$ odd, indicates that the magnetic mode is of type $G$.[8] In this mode the six nearest neighbors of a spin are antiparallel to it. Since a cubic lattice (with $a = 2a_0$) is consistent with the powder-diffraction data, all spin directions are equivalent.[9] Therefore we are not able to give, on the basis of these data, any information regarding the spin direction. By extrapolating Fig. 2(b), the magnetic contribution to the {211}+{103} line was estimated. From this contribution and from the {101} intensity a magnetic moment of $(4.7 \pm 0.2)\mu_B$ was calculated for the manganese ions.

Kestigian[4] reported that for $TlMnCl_3$ below 30 °C, $c_0/a_0 = 5.04/5.02 = 1.004$. This distortion is too small to be observed in our neutron-diffraction patterns [Figs. 1(b) and 1(c)]. A similar situation was reported for $KMnF_3$: Low-temperature (4.2 °K) neutron diffraction discussed by Scatturin *et al.*[2] and low-temperature ($T < 95$ °K) x-ray diffraction seen by Beckman and Knox[10] showed the compound to be orthorhombic with *Pbnm* as the most probable space group. Differences of up to 0.7% between $a$ and $c$ were observed. No splitting of diffraction lines was, however, observed in the neutron-diffraction pattern of $KMnF_3$. $TlMnCl_3$ and $KMnF_3$ are similar in many respects: The Goldschmidt tolerance factor $t$[11] equals 0.89 for $TlMnCl_3$ and 0.88 for $KMnF_3$. In both materials a departure from

TABLE II. Effect of an external magnetic field of 6 kG applied parallel to the scattering vector. The indices correspond to the tetragonal crystallographic cell with $a = b = 5.02 \times \sqrt{2}$ Å, $c = 5.02 \times \sqrt{2}$ Å. $N$ is the number of counts including the background $B$ without applied magnetic field. $\Delta N$ is the change in the number of counts due to the application of the magnetic field.

| {hkl} | $N$ | $\Delta N$ | $100\Delta N/(N-B)$ |
|---|---|---|---|
| 101 | 48 330 | +12 356 | +41[a] |
| 210 | 44 991 | − 527 | − 2.5 |
| 211, 103 | 47 887 | +7 989 | +45[a] |
| 202 | 53 259 | − 213 | − 0.4 |
| 212 | 51 600 | − 937 | − 3 |
| 220, 004 | 51 381 | + 2 928 | +7 |
| 400, 224, 041, 025 | 49 561 | − 2 135 | − 6 |
| 410, 411, 323, 215, 402<br>006, 330, 314, 331 | 48 524 | +1 888 | +8 |
| 324, 305, 413, 206, 422<br>333, 315, 216 | 49 153 | − 89 | − 0.2 |

[a] Related to the magnetic contribution.

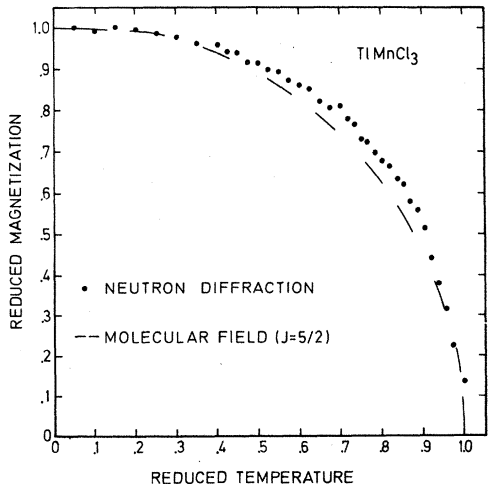


FIG. 3. Reduced temperature dependence of the reduced sublattice magnetization derived from the magnetic reflection {101}. The reduced magnetization calculated in the molecular-field approximation for $J = \frac{5}{2}$ is also shown.

TABLE III. Observed and calculated integrated intensities for $TlMnCl_3$ at 4.2 °K. Indices correspond to the tetragonal crystallographic cell $a=b=5.02\times2$ Å, $c=5.02\times2$ Å. The calculated magnetic contribution (if different from zero) is given in parentheses and is included in $I_{calc}$.

| $\{hkl\}$ | $I_{obs}$ | $I_{calc}$ |
|---|---|---|
| 101 | 8.5 | 8.6 (7.1) |
| 110, 002 | 1.2 | 0.8 |
| 111 | 0 | 0 |
| 112, 200 | 1.6 | 1.1 |
| 021 | 0 | 0 |
| 210 | 1.6 | 1.5 |
| 211, 103 | 6.9 | 6.6 (3.7) |
| 202 | 31.8 | 30.8 |
| 113 | 0 | 0 |
| 212 | 2.5 | 2.1 |
| 220, 004 | 10.7 | 10.5 |
| 311 | 0 | 0 |
| 400, 224, 041, 025 | 7.9 | 8.1 |
| 410, 411, 323, 215, 402<br>006, 330, 314, 331 | 6.4 | 7.4 (0.6) |
| 412, 420, 332, 225, 116<br>043, 421 | 2.1 | 3.2 |
| 324, 305, 413, 206, 422<br>333, 315, 216 | 18.7 | 19.3 (0.1) |

$Pm3m$ (ideal perovskite) is observed above the Néel temperature.[12] In the low-temperature neutron-diffraction patterns relatively strong distortion lines are observed at both sides of the $\{202\}$ line.[2] At low temperatures both materials order antiferromagnetically in mode $G$, and below the Néel temperature a transition to weak ferromagnetism is observed. In view of this similarity, and because the space group $Pbnm$ is encountered also in many other distorted perovskites,[7] an attempt was made to analyze the data of $TlMnCl_3$ on the basis of this space group.

At low temperatures the distortion contributions become more pronounced (Figs. 1 and 2). Accordingly, the calculations were carried out for data taken at liquid-helium temperature. A least-squares calculation for the parameters of the ionic sites led to calculated intensities which fitted the observed intensities with an $R$ factor[5] of 6%. The observed and calculated intensities are presented in Table III. Practically only the chlorine ions were found to be shifted from their ideal positions. The thallium ions retained their ideal positions. The intensities in Table III were calculated with the following positions of the ions in the space group $D_{2h}^{16}$-$Pbnm$:

Tl : $(4c)\pm(x, y, \frac{1}{4};\ \frac{1}{2}-x, \frac{1}{2}+y, \frac{1}{4})$ with $x=y=0$;

Mn : $(4b)\ \frac{1}{2}, 0, 0;\ \frac{1}{2}, 0, \frac{1}{2};\ 0, \frac{1}{2}, 0;\ 0, \frac{1}{2}, \frac{1}{2}$;

$Cl_I$ : $(4c)$ with $x=0.09$, $y=\frac{1}{4}$;

$Cl_{II}$ : $(8d)\pm(x, y, z;\ \frac{1}{2}-x, \frac{1}{2}+y, \frac{1}{2}-z;$

$\bar{x}, \bar{y}, \frac{1}{2}+z;\ \frac{1}{2}+x, \frac{1}{2}-y, \bar{z})$

with $x=0.71$, $y=0.27$, $z=0$.

The magnetic contribution was calculated for mode $G$ with a magnetic moment of $4.7\mu_B$. The chlorine parameters are estimated to be accurate within ± 0.02.

As already mentioned we cannot deduce the spin direction from the neutron-diffraction measurements. However, the occurrence of a weak ferromagnetic moment, which was deduced from the VSM measurements, implies that the spins are directed either in the $x$ or in the $z$ direction, because in the irreducible representations of $Pbnm$ $G_y$ is not compatible with a weak ferromagnetic moment.[8]

The analysis presented above was based on a clear distinction between magnetic and distortion contributions. The distinction was corroborated by the results obtained by the application of external magnetic fields to the samples. To show this we note that as a result of the application of an external magnetic field parallel to the scattering vector, the antiferromagnetically ordered spins tend to align perpendicular to the applied field. Also, a weak ferromagnetic moment, if present, will tend to bring the antiferromagnetic ordered spins into the reflecting plane because in any of the irreducible representations of $Pbnm$ the ferromagnetic component (if any) is perpendicular to the antiferromagnetic component.[8] The accompanied maximal (i.e., at saturation) expected change in intensity corresponds to an increase in $q^2$ from $\frac{2}{3}$ to 1.[9] It is seen from Table II that in the two lines with $h+k$ odd and $l$ odd an increase of over 40% was observed. The small changes observed in some of the other lines may be due to magnetostriction effects.

ACKNOWLEDGMENTS

The authors wish to thank Professor S. Shtrikman of the Weizmann Institute of Science and Dr. Z. H. Kalman of the Hebrew University for many helpful discussions.

[1]John B. Goodenough, *Magnetism and the Chemical Bond* (Interscience, New York, 1963), p. 221.

[2]V. Scatturin, L. Corliss, N. Elliott, and J. Hastings, Acta Cryst. 14, 19 (1961).

[3]H. F. McMurdie, J. de Groot, M. Morris, and H. E. Swanson, J. Res. Natl. Bur. Std. 73A, 621 (1969); D. J. Ijdo, thesis, University of Leiden, 1960 (unpublished).

[4]Z. H. Kalman, A. Zodkevits, and J. Makovsky, Israel J. Chem. 7, (1969); see also M. Kestigian, Materie Res. Bull. 5, 263 (1970).

[5]$R$ is given by $R=(\sum|I_{obs}-I_{calc}|/\sum I_{obs})\times100$.

[6] $B$ is defined by $I_{obs}=I_{calc}\ e^{-B/2d^2}$.

[7] Ralph W. G. Wyckoff, *Crystal Structures*, 2nd ed. (Interscience, New York, 1964), Vol. II, p. 390.

[8] E. F. Bertaut, Acta Cryst. A24, 217 (1968).

[9] G. Shirane, Acta Cryst. 12, 282 (1959).

[10] O. Beckman and K. Knox, Phys. Rev. 121, 376 (1961).

[11] $t$ is given by $(R_A+R_x)/\sqrt{2}\ (R_B+R_x)$, where $R_A$, $R_B$, and $R_x$ are the ionic radii.

[12] Minkiewicz *et al.* [V. J. Minkiewicz, Yasuhiko Fujii, and Yasusada Yamada, J. Phys. Soc. Japan 28, 443 (1970)] found $KMnF_3$ to be of symmetry $I4/mcm$ or $Ibmm$ at the temperature range $125 < T < 180$ °K. Our data, on the other hand, are inconsistent with the $I$ lattice throughout the temperature range $4.2 < T < 272$ °K.

PHYSICAL REVIEW B VOLUME 3, NUMBER 7 1 APRIL 1971

# Energy Transport at Finite Temperatures in Isotropic Magnetic Chains with $S = \frac{1}{2}$

D. A. Krueger
*Department of Physics, Colorado State University, Fort Collins, Colorado* 80521

(Received 12 October 1970)

Energy transport is shown to be nondiffusive at finite temperatures in a magnetic chain of spin-$\frac{1}{2}$ particles with isotropic nearest-neighbor Heisenberg interactions in zero external field. In a uniform magnetic field, the Zeeman energy ensures that energy diffusion is reestablished at all temperatures if spin diffusion is present. At infinite temperatures the introduction of weak next-nearest-neighbor interactions also reestablishes energy diffusion. We use the Mori-Kawasaki expression for the diffusion constant in terms of the second and fourth moments of the time Fourier transform of the relaxation function. Investigation of the sixth moment indicates that the time derivative of the energy density exhibits diffusive behavior even though the energy density does not.

It has been shown[1] that, at infinite temperatures, energy transport is nondiffusive in an isotropic magnetic chain of spins with $S = \frac{1}{2}$ and zero external field. In this paper we show it is true at all temperatures if one uses an approximate expression for the inverse decay time based on the second and fourth moments of the energy relaxation function.

The Hamiltonian for our system is

$$H = -2J\sum_{n=0}^{N-1}\vec{S}_n\cdot\vec{S}_{n+1} + \mathcal{H}\sum_{n=0}^{N-1}S_n^z = H_x + H_z\ , \tag{1}$$

where $H_x$ is the exchange energy and $H_z$ is the Zeeman energy. The relevant relaxation function for energy transport at finite temperature is

$$R(k,t) = \{h(k,t)\,,\ h(-k,0)\}\ \{h(k,0)\,,\ h(-k,0)\}^{-1}, \tag{2}$$

where $h(k,t)$ is the Fourier transform of the energy density

$$h(k,t) = \sum_n e^{ikan}h_n(t)\ ,$$

$$h_n(t) = -J[\vec{S}_n(t)\cdot\vec{S}_{n+1}(t) + \vec{S}_n(t)\cdot\vec{S}_{n-1}(t)] + \mathcal{H}S_n^z(t)\ , \tag{3}$$

$$\{A,B\} = \int_0^\beta d\lambda\ \langle e^{\lambda H}A\,e^{-\lambda H}B\rangle - \beta\langle A\rangle\langle B\rangle\ ,$$

and

$$\langle O\rangle = \mathrm{Tr}\,e^{-\beta H}O/\mathrm{Tr}\,e^{-\beta H}\ .$$

The lattice constant is $a$ and $\beta = (k_BT)^{-1}$ where $k_B$ is Boltzmann's constant and $T$ is the temperature. If diffusion is present, then for small $k$ the time dependence of $R(k,t)$ is approximately[2]

$$R(k,t) = \exp[-|t|\Gamma(k)]. \tag{4}$$

As discussed in Ref. 3, an approximate expression for $\Gamma(k)$ is

$$\Gamma(k) = [\pi/2]^{1/2}M_2(k)[M_2(k)/M_4(k)]^{1/2}, \tag{5}$$

where

$$M_{2n}(k) = \left[\left(\frac{1}{i}\frac{\partial}{\partial t}\right)^{2n}R(k,t)\right]_{t=0}\ . \tag{6}$$

Energy diffusion is said to occur when the average of the energy density $\bar{h}(r,t)$, obeys a diffusion equation for long-wavelength disturbances

$$\frac{\partial}{\partial t}\bar{h}(r,t) = D\nabla^2\bar{h}(r,t)\ .$$

This implies that $\Gamma(k)$ is $Dk^2$ for small $k$. $D$ is the diffusion constant. For zero external field, we shall show $M_2(k) = k^2a(k)$ and $M_4(k) = k^4b(k)$ for small $k$. In addition, $a(0)$ is shown to be finite at infinite temperatures, and $b(0)$ is proved to be finite for all temperatures. Thus one expects $\Gamma$ to be proportional to $k$ for small $k$ in contrast to the $k^2$ dependence for diffusion.

Convenient expressions for the required moments are

$$M_2(k) = C(k)^{-1}\sum_n e^{ikan}\{[H,\ [H,h_n]],\ h_0\}\ , \tag{7}$$

$$M_4(k) = C(k)^{-1}\sum_n e^{ikan}\{[H,\ [H,[H,h_n]]],[H,[H,h_0]]\}\ , \tag{8}$$